



Published in final edited form as:

*J Am Chem Soc.* 2011 May 4; 133(17): 6587–6595. doi:10.1021/ja108807j.

## The Impact of Distinct Chemical Structures for the Development of a Methamphetamine Vaccine

Amira Y. Moreno, Alexander V. Mayorov, and Kim D. Janda\*

Departments of Chemistry and Immunology, the Skaggs Institute for Chemical Biology and the Worm Institute of Research and Medicine (WIRM); The Scripps Research Institute. 10550 N. Torrey Pines Road, La Jolla, California 92037, USA

### Abstract

(+)-Methamphetamine (METH) use and addiction has grown at alarming rates over the past two decades, while no approved pharmacotherapy exists for its treatment. Immunopharmacotherapy has the potential to offer relief through producing highly specific antibodies that prevent drug penetration across the blood-brain barrier thus decreasing reinforcement of the behavior. Current immunotherapy efforts against methamphetamine have focused on a single hapten structure, namely linker attachment at the aromatic ring of the METH molecule. Hapten design is largely responsible for immune recognition as it affects presentation of the target antigen and thus the quality of the response. In the current paper we report the systematic generation of a series of haptens designed to target the most stable conformations of methamphetamine as determined by molecular modeling. Based on our previous studies with nicotine, we show that introduction of strategic molecular constrain is able to maximize immune recognition of the target structure as evidenced by higher antibody affinity. Vaccination of GIX<sup>+</sup> mice with six unique METH immunoconjugates, resulted in high antibody titers for three particularly promising formulations (45–108 µg/mL, after second immunization) and high affinity (82, 130 and 169 nM for MH2, MH6 and MH7 hapten-based vaccines, respectively). These findings represent a unique approach to the design of new vaccines against methamphetamine abuse.

### Keywords

methamphetamine; active vaccination; immunopharmacotherapy; constrained hapten

### INTRODUCTION

(+)-Methamphetamine (METH) use and addiction in the United States has grown at alarming rates over the past two decades,<sup>1</sup> burdening the US economy with an estimated medical, lost productivity, and law enforcement cost of \$23.4 billion.<sup>2</sup> The effect of methamphetamine on the dopaminergic signaling pathway is largely responsible for its powerful rewarding<sup>3</sup> as well as addictive properties. Furthermore, the high rate of relapse in the patients undergoing methamphetamine withdrawal underscores the level of challenge in development of an effective therapy for methamphetamine addiction.<sup>4</sup> Currently, psychosocial and behavioral management is the only available treatment.

\* kdjanda@scripps.edu .

**SUPPORTING INFORMATION PARAGRAPH.** Complete synthetic routes and characterization of chemical compounds as well as binding competition curves are provided. This material is available free of charge via the internet at (<http://pubs.acs.org/page/jacsat/submission/authors.html>).

Development of an efficacious pharmacotherapy is of pressing concern, yet, the complexity of drug action on the brain circuitry has presented a significant challenge.<sup>5</sup> Immunopharmacotherapy uses an alternative approach wherein antibodies are used to prevent drug distribution to brain receptors thus decreasing reinforcement of the behavior. Previous immunotherapy efforts have targeted various drugs of abuse<sup>6</sup> and importantly, anti-nicotine<sup>7</sup> and anti-cocaine vaccines<sup>8</sup> have shown titer dependent efficacy during clinical trials. Active vaccination efforts against METH have largely proven ineffective during behavioral testing,<sup>9</sup> providing an impetus for development of more effective approaches to a vaccine against methamphetamine addiction.

The success of any small molecule active vaccine is intimately determined by three factors; antibody specificity, affinity and antibody concentration (titer). Small molecules, such as METH, require appendage to carrier macromolecules in order to elicit an immune response. The chemical positioning of a linker to the target antigen has proven to be crucial for proper immune stimulation both in terms of amount of antibody elicited and antibody specificity.<sup>10</sup> Thus, proper hapten design is critical for immune recognition as it affects presentation of the target antigen and thus quality of the response.<sup>10-11</sup> Immunotherapy efforts against methamphetamine have largely focused on the use of a single scaffold, i.e. linker attachment at the aromatic ring of the parent molecule (Figure 1).<sup>12</sup> Variations of linker identity and length has allowed for some immune regulation, yet vaccination of this structure has proven largely ineffective during behavioral testing.<sup>9</sup> The sole exception is a METH vaccine based on a self-adjuvanting peptide construct wherein efficacy was independent of hapten design and was determined by the presence of an additional T cell epitope from Tetanus Toxin.<sup>13</sup>

Based on the poor response obtained from active vaccination, the bulk of the literature to date has focused on the use of anti-METH monoclonal antibodies, i.e. passive vaccination, which when administered has shown reduction of METH associated behavior.<sup>14</sup> Despite this potential efficacy, the expense of passive vaccination is of concern. Active vaccination generates immunological memory to repeated exposure of the drug conjugate. Thus, the cost effectiveness of treatment is increased allowing for longer sustained protection with minimal compliance and could be a viable approach for relapse prevention.

As a path forward for the development of a METH vaccine, we report the systematic generation of a series of unique chemical structures designed to target the most stable conformations of methamphetamine in solution as determined by molecular modeling. We present the serological analysis of GIX<sup>+</sup> mice following vaccination with six unique METH haptens, with three of them being particularly promising, and elaborate on the impact of these findings on the design of future vaccines against methamphetamine abuse.

## RESULTS AND DISCUSSION

### Theoretical Calculations

Vital to constrained hapten design, the conformational profile of the protonated form of (+)-methamphetamine was examined using MacroModel 9.1 equipped with Maestro 7.5 graphical interface (Schrödinger, USA). Structures were minimized using the OPLS\_2005 force field<sup>15</sup> and the Polak-Ribiere conjugate gradient. Aqueous solution conditions were simulated using the continuum dielectric water solvent model (GB/SA).<sup>16</sup> The key dihedral angles in these simulations were denoted as  $\Phi$  ( $C^1-N-C^2-C^3$ ) and  $\Psi$  ( $N-C^2-C^3-Ph$ ). As expected, two dihedral drive simulations on the global minimum of the methamphetamine structure showed the lowest energy conformation positioned the largest substituents *anti*- to one another ( $\Phi \approx 180^\circ$ ,  $\Psi \approx 180^\circ$ ) with two separate *gauche-anti* conformers ( $\Phi \approx 180^\circ$ ,  $\Psi \approx \pm 60^\circ$  and  $\Phi \approx \pm 60^\circ$ ,  $\Psi \approx 180^\circ$ ) also identified as potential energy sinks (Figure 2). These findings allowed us to identify two approaches to constructing conformationally constrained

methamphetamine haptens: 1) C<sup>1</sup>-C<sup>4</sup> constraint and 2) C<sup>1</sup>-phenyl ring constraint (Figure 3). The former approach was convenient to achieve by using a commercially available appropriately ornamented piperazine template, while the tetrahydroisoquinoline (THIQ) template was found to be suitable for establishing the latter type of dihedral constrain, both by matching the dihedral angles of the energetically favored ( $\square$ )*gauche-anti* conformer ( $\Phi \approx -60^\circ$ ,  $\Psi \approx 180^\circ$ ), and by possessing a sufficient basicity of the requisite secondary amine nitrogen. Thus, the designed haptens fall into one of three categories as determined by the identity of their core structures. MH1 and MH2 present an inherently *anti-anti* constrained piperazine nucleus, MH3 and MH5 are derivatized tetrahydroisoquinolines and finally MH6 and MH7 are functionalized versions of the unconstrained methamphetamine molecule (Figure 4).

The global minima of (+)-methamphetamine and the hapten core structures MH1-3, MH5-7 (in their respective protonated forms) were obtained using the hybrid Monte Carlo/Low Frequency Mode simulations (MCMM/LMCS) procedure as implemented in Macromodel<sup>17</sup> using the energy minimization routine as described above. To simplify the computational experiments and the subsequent comparison of structures, the alkylsulfhydryl linker HS-(CH<sub>2</sub>)<sub>4</sub>- was removed in the simulations of all hapten structures, except for MH6, where only the terminal sulfhydryl group was removed. Superpositions of the minimized parent molecule with all haptens were performed by alignment of four key loci; namely the amine nitrogen, the *N*-Me, C<sup>2</sup>-, and C<sup>3</sup>-carbon atoms. Superpositions of the constrained haptens MH1(R) and MH2(R), as well as, unconstrained haptens MH6(S) and MH7(S) with the global minimum conformation of methamphetamine showed an excellent fit (Figures 5 and 6). Similarly, MH3(S) and MH5(R) structures were determined to share a matching core conformation with the (-) *gauche-anti* conformer of methamphetamine (Figure 7). Thus, each of the two constrained core categories mimics a distinct low energy conformation of the target structure. Deviations in conformation for all superpositions were calculated as a root mean square (RMS) and were found to be reasonably low at < 0.15, indicating a good fit.

It is important to point out that we considered the presence of basic secondary amine functionality in our haptens to be vital for the success of the methamphetamine vaccine. While the basicity of the acyl-piperazine core-based haptens MH1 and MH2 (pK<sub>a</sub> = 11.123 for piperidine, 9.82 for piperazine)<sup>18</sup> was expected to be similar to that of methamphetamine (pK<sub>a</sub> = 10.1),<sup>19</sup> the ionization constant of the THIQ template has been shown to be somewhat lower (pK<sub>a</sub> ≈ 9.30).<sup>20</sup> We hypothesized that both core structures were basic enough to ensure sufficient protonated state population at the physiological pH (7.4), giving rise to antibodies targeting the methamphetamine structure in its protonated form. A possible complication from using a basic amine linker in MH5 hapten was recognized, due to the uncertainty of its protonation behavior. Using the NMR work of Beaumont and co-workers on the structurally related aminomethyl-THIQ analogues<sup>20</sup> as a guide, we concluded that the linker nitrogen should be expected to be somewhat more basic than the THIQ core nitrogen (pK<sub>a</sub> (dimethylamine) = 10.73 vs pK<sub>a</sub> (THIQ) = 9.3).<sup>18</sup> Computational pK<sub>a</sub> prediction as implemented in Schrodinger Epik program<sup>21</sup> supported this hypothesis, yielding the pK<sub>a</sub> estimates at 9.62 for the linker amino group, and 6.72 for the THIQ core. Regardless, comparison of the global minima of both protonated forms showed near identical conformations (RMSD = 0.055) (not shown). In addition, as pointed out by Beaumont and co-workers<sup>20</sup>, intramolecular hydrogen bonding between the protonated and the free amino groups is likely, and was in fact found by the computer simulations in both protonated forms (Figure 8), which suggested a certain degree of proton sharing between the amino groups, which we deemed both acceptable and interesting to pursue as a structural feature of a methamphetamine hapten.

## Hapten Design

Our strategy for hapten design consisted of three main veins: 1) to focus the response on the lowest energy conformations of methamphetamine as elucidated by molecular modeling, 2) to mimic the most psychoactive enantiomer of the parent molecule, and 3) to maximize hapten loading efficacy via a non-competing bioconjugation technique.

First, we hypothesized that targeting of the lowest energy conformations could be achieved by either a constrained or unconstrained approach. Unconstrained structures would effectively mimic the target by theoretically converging onto the same energy conformation of the parent structure. However, depending on the energy expenditure required to go from one potential energy sink to another, a series of structures could exist through time. Previous reports on development of small molecule haptens for vaccines against nicotine abuse have provided compelling evidence that application of conformational constraints can be used to reduce the hapten's internal rotational degree of freedom, thus minimizing the entropic loss upon antibody binding.<sup>6a, 22</sup> Methamphetamine, like nicotine, is a small molecule with ample degrees of freedom provided by rotation along its sigma bonds. Thus, we hypothesized that rational introduction of a strategic molecular constrain would be able to "guide" the immune response towards the most stable, and thus, most prevalent conformation of the parent structure. Based on our modeling experiments, *vide supra*, we proposed two specific ways to introduce molecular constraint in order to target two distinct low energy conformations for methamphetamine. This allowed us to categorize our haptens based on the identity of their core structures. MH1 and MH2 present a constrained piperazine nucleus, MH3 and MH5 are constrained based on a tetrahydroisoquinoline scaffold and finally MH6 and MH7 are linker functionalized versions of the free rotating methamphetamine molecule.

Second, it is well established in the literature, that (+)-methamphetamine is about five times more potent stimulant drug than its (–)-methamphetamine enantiomer, thus increasing its liability for abuse.<sup>23,24</sup> During our hapten design, we hypothesized that paying special attention to the stereochemical requirements of the more potent enantiomer of methamphetamine would allow for superior immune tuning. Thus, the design of our haptens focused on targeting the appropriate (+)-configuration.

Finally, we hypothesized that maximizing hapten load onto the carrier proteins could provide more potent immune stimulation. Previous work focused on the use of carbodiimide activation of carboxylic acid haptens for attachment to free amino groups in the lysine residues of carrier proteins.<sup>9</sup> Yet, we argue that this type of chemistry may not be optimal when dealing with a structure, like methamphetamine, which itself presents a reactive secondary amine. This could lead to loss of material to oligomerizations-type reactions as well as unreliable conjugation. We have opted instead for an orthogonal conjugation technique using a maleimide spacer with pH-modulated thiol selectivity. The robustness of this conjugation method is highlighted by similar conjugation efficiencies for all haptens tested, determined by the number of hapten copies on the carrier, which we suspected to have an impact on the efficacy of immune stimulation towards a particular target. Efficacy of conjugation was monitored using MALDI-TOF MS for hapten coupling to bovine serum albumin (BSA) under the same conditions, and all haptens were found to produce similar coupling rates at 24–29 copies per BSA molecule.

## Synthetic preparation of haptens

All haptens were prepared from commercially available starting materials using standard reaction conditions. Full synthetic details and characterization of all haptens is given in the Supporting Information. We note that whenever possible we obtained enantiomerically pure

materials to match the most active stereoisomer of methamphetamine. However, MH1, MH3 and MH5 were synthesized in racemic form and were not further resolved. Additionally, MH3 yielded two regioisomers that were not separated further, as they only vary at the site of linker attachment within the aromatic ring, (positions 6 and 7, Supporting Information). Molecular modeling of both regioisomers deemed this not to be critical for immune presentation. A brief description of each synthesis is shown, *vide infra*.

MH1 and MH2(R), constrained *anti-anti* METH mimetics, were synthesized by functionalization of the commercially available piperazine cores with the appropriate linker, 6-(tritylthio)hexan-1-amine for MH1 and 6-(tritylthio)hexanoic acid for MH2. Carbodiimide activation chemistry was used for linker coupling; this was followed by acid deprotection of the trityl group to yield the desired haptens (Scheme 1). In short, we took advantage of the fact that the piperazine core needed to prepare MH2 was commercially available as either enantiomer thus allowing easy access to structures that targeted both the (+) and (–) enantiomers of methamphetamine. This was significant as it would allow us to gauge the importance of retaining the stereochemical requirements of our target, (+)-methamphetamine, the most active isomer, during hapten design. In contrast for the MH1 hapten, starting material was only available for the opposite enantiomer, thus to access both isomers, racemization was accomplished using 1,8-Diazabicycloundec-7-ene (DBU) and heat (see Supporting Information). The two isomers of MH1 were not further resolved as we have previously shown how the immune system can readily generate antibodies able to selectively recognize either antipode from a racemic synthetic hapten.<sup>25</sup>

The syntheses of tetrahydroisoquinoline (THIQ) haptens MH3 and MH5 are shown within scheme 2. The synthesis of MH3 was initiated with indium catalyzed reduction of 3-methyl isoquinoline to the corresponding 1,2,3,4-tetrahydroisoquinoline, **1**; this was followed by aromatic nitration, which resulted in **2** as a mixture of regioisomers at positions 6 and 7, as stated, *vide supra*, that were not further resolved. Boc-protection of the reactive secondary amine of **2** followed by reduction of the nitro moiety granted **3**, and allowed for facile coupling of the 6-(tritylthio)hexanoic acid linker. Global acidic deprotection provided MH3. The synthesis of MH5 was initiated with the reduction and re-oxidation of the carboxylic acid from commercially available (R)-N-BOC-1,2,3,4-tetrahydroisoquinoline-3-carboxylic acid (Fluka), providing **5**. Aldehyde **5** was subjected to reductive amination using sodium cyanoborohydride and 6-(tritylthio)hexan-1-amine; this was followed by global acidic deprotection to yield MH5.

The synthesis of the unconstrained hapten cores proceeded in the following manner. MH6 was accessed by simple N-alkylation of (+)-amphetamine with 6-(tritylthio)hexyl methanesulfonate followed by acid deprotection. The synthesis of MH7 was more involved and began from (+)-methamphetamine that was found to be quite volatile as its free base thus requiring protection of the secondary amine with trifluoroacetic anhydride in order to allow for easier handling. Thus, aromatic nitration gave rise to *para*-substituted trifluoroacetamide methamphetamine, **6**, as the major product, which was separated using silica chromatography. Reduction of the nitro functionality yielded **7**, which was followed by linker coupling using 6-(tritylthio)hexanoic acid providing **8**. Base/acid deprotection of the trifluoroacetamide and trityl moieties gave the final product MH7.

### Characterization of anti-METH antibodies

As stated, success of active vaccination is contingent upon both the magnitude of the response as well as the affinity and specificity of the antibodies (Abs) generated. The magnitude of the immune response was initially assessed by ELISA on microtiter plates coated with either MH6 or MH7-BSA conjugates. It was immediately apparent that the site of linker attachment played an important role in determining relative cross reactivity, i.e.

MH3 preferentially saw MH7, while MH5 preferentially identified MH6. This bias was removed by use of equilibrium dialysis; a solution based assay we feel more closely resembles the *in vivo* interaction. All binding constants as well as antibody concentrations reported were calculated from a solution based radioimmunoassay (RIA) and normalized thus, allowing for direct comparison of values between test groups.

We hypothesized that mimicking of the target structure via either introduction of strategic molecular constrain or effective functionalization would maximize immune recognition of the target structure as evidence by higher antibody affinity and specificity. Gratifyingly, the highest affinity anti-METH Abs were observed with constrained hapten MH2(R), an *anti-anti* METH mimetic as determined by molecular modeling, followed by unconstrained haptens MH6 and MH7. By the end of the study, polyclonal responses had an affinity well within the range of previous anti-methamphetamine mAbs tested (10–250 nM).<sup>26</sup> Nonetheless, unconstrained haptens MH6 and MH7 produced antibody concentrations in the 150–220  $\mu\text{mL}$  range which corresponds to 3 $\times$  and 2 $\times$  larger responses than constrained hapten MH2(R). To put these values into perspective, a nicotine vaccine that has advanced to clinical trials generated antibodies in rats within the same range (184  $\mu\text{g/mL}$ ).<sup>27</sup> Furthermore, these values are about two orders of magnitude higher than those reported by Duryee et al.<sup>13</sup> wherein vaccination showed moderate effects in the rates of methamphetamine intravenous self-administration. On the other hand, vaccination with MH1 as well as the tetrahydroisoquinoline haptens (THIQ) MH3 and MH5 produced antibodies with minimal affinity for METH in solution (>50 $\mu\text{M}$ ) and thus were discarded from future testing.

These findings suggest that targeting the (–)*gauche/anti* conformation of methamphetamine does not appear to be as effective at raising an immune response against the global minimum *anti/anti* conformation. Among the possible reasons for the apparent inability of the tetrahydroisoquinoline (THIQ) hapten (MH3 and MH5)-based vaccines to raise sufficient antibody titers, the lower pKa of the requisite secondary amino group appears to offer one plausible explanation. Furthermore, it seems reasonable to conclude that positioning of the aromatic ring is also a critical determinant of efficacy. In the case of MH1, a similar *anti-anti* METH mimetic as MH2, the steric repulsion between the aromatic group and the carbonyl group of the MH1 2-piperazinone template resulted in a misalignment of the aromatic ring as compared to the global minimum structure of METH, and in contrast to MH2, which showed a near-perfect fit (Figure 5). Thus, the better fit of the MH2 hapten structure with the global minimum conformation of methamphetamine seems to correlate with the higher titers produced with this hapten. This rationale is further supported by the fact that 1) both of the THIQ haptens which showed poor efficacy also see a misalignment of their aromatic moiety with that of the target structure and 2) both unconstrained haptens, whose minima structures showed a better fit with that of METH, showed a measurable immune response (Figures 6 and 7).

We note that in contrast to what was expected, bleeds following a third injection showed reduced antibody concentrations. Additional booster injections are usually expected to increase the magnitude of the response as well as focus the antibody population towards the preferred target. In our case antibody affinity was greatly increased for MH2(R) and MH6 yet remained the same for MH7 across both bleeds. We interpret the decrease in antibody concentration in one of two ways. It is possible that the immune response prior to the last injection was still in the top part of the bell shape curve and thus upon antigen presentation part of the current stock of circulating antibodies went to “neutralize the infection” thus reducing the overall antibody concentration. Alternatively, it is possible that overall antibody count was lowered in favor of increasing antibody affinity. We suspect an

optimized vaccination schedule wherein animals are allowed a longer “rest” period between injections would be able to rule in favor of one hypothesis.

Amphetamine (amph) is a closely related drug of abuse as well as a METH metabolite, thus the binding affinity of the antisera for this drug is of interest and was also assayed. Ideally, a clinically viable METH vaccine would produce a response able to provide good recognition for both related structures, thus maximizing its protective effects. Obtaining anti-METH antibodies that cross-react with amphetamine has historically been a challenge with the traditional hapten design, i.e. linker attachment at the aromatic moiety.<sup>28</sup> Gratifyingly, the antisera of MH2(R) (*anti-anti* constrained METH mimetic) and MH6 (unconstrained hapten) vaccinated animals had moderate affinity for amphetamine which improved upon boosting. MH7, consistent with what has been typically observed with this hapten design<sup>28</sup>, had overall poor affinity (Table 1). The differences for amphetamine cross reactivity between MH6 and MH7, both unconstrained cores, is not obvious based on our modeling and is likely the result of an unintended linker effect.

In order to test the importance of retaining the stereochemical requirements of the more potent enantiomer of methamphetamine during hapten design, we synthesized the opposite (S)-enantiomer for the best constrained hapten MH2 (a piperazine core, *anti-anti* METH mimetic). The response elicited from immunization with MH2(S) was assayed for relative affinity to both isomers of METH. The first bleed contained Abs with little (+)-METH affinity thus making it difficult to quantify. Gratifyingly, the 2<sup>nd</sup> bleed antisera of MH2(S) immunized mice had six times better affinity for the (–)-METH isomer as predicted by molecular modeling (Table 2). Furthermore, to prove if stereochemical requirements were also critical for unconstrained METH mimetics, the affinity of MH6 (modeled after (+)-METH) antisera for (–)-METH was measured. MH6 was chosen over MH7 due to its higher antibody concentrations as well as lower binding constants for both METH and AMPH. Competitions with (–)-METH show that MH6 preferentially bound (+)-METH by at least 10 fold (Table 2).

## CONCLUSIONS

In summary, the current paper details the rational design of six METH haptens, five with unique structural characteristics, and their ability for precise generation of anti-METH immune responses. Three haptenic compounds, MH2(R), MH6 and MH7, show particular promise in generation of a potentially clinically relevant METH vaccine based on both an elevated antibody titer as well as nanomolar range (+)-METH affinity. Introduction of strategic molecular constraint and stereochemical requirements in MH2(R) allowed for generation of a polyclonal response well within the range of previous monoclonal antibodies tested. Additionally, MH2(R) generated antibodies with moderate affinity for amphetamine, a related drug and methamphetamine metabolite. However, magnitude of the response remained highest in the two unconstrained structures MH6 and MH7. MH6 is of particular interest as not only did it present a surprisingly high antibody concentration but it also showed good specificity towards METH and discreet affinity towards amphetamine. Further studies including improvements onto the adjuvant activity of the formulations as well as behavioral studies with our prime hapten leads will provide a practical approach toward development of a clinically useful vaccine against methamphetamine abuse.

## MATERIALS AND METHODS

### Synthetic generation of methamphetamine haptens

Synthetic details for the three haptens of interest are detailed below. Full synthetic detail and characterization of all haptens is given in the Supporting Information.

### Synthesis of MH2(R)

(R)-1-Boc-2-Benzylpiperazine was purchased from Synthonix and used without further purification. 0.153mmol of 6-(tritylthio)hexanoic acid were mixed with 0.2mmol EDC and 0.046mmol DMAP in 0.7mL DCM. 0.184mmol of (R)-1-Boc-2-Benzylpiperazine and 0.3mmol 4-methyl morpholine were added and reaction was allowed to stir under argon at room temperature for 3 hours. The mixture was diluted with ethyl acetate and the organic layer washed 3× with saturated sodium bicarbonate, 3× with 10% citric acid and 1× with water. The organic layer was then dried over sodium sulfate and rotovaped. The residue was then passed through a short plug of silica using 80% ethyl acetate/hexane as eluent. The crude product was used without further purification. Global deprotection was achieved by addition of trifluoroacetic acid in a 1:1 dilution with DCM. Drops of triisopropylsilane were added to scavenge the trityl groups. After 2 hrs, the mixture was rotovaped and purified by preparative HPLC. Method = 0–5min 30%B, to 33%B over 2 min, to 40% B over 27min, to 95%B over 5 min, hold for 10min, requilibrate. Product retention time = 13min. Experimental Yield over 2 steps = 56%. Observe amide rotamers on NMR. <sup>1</sup>H NMR (600 MHz, MeOD) δ 7.44 – 7.24 (m, 13H), 4.58 (s, 1H), 4.44 (s, 1H), 4.08 (d, *J* = 14.4 Hz, 1H), 3.95 (d, *J* = 14.5 Hz, 1H), 3.54 (dd, *J* = 15.6, 12.2 Hz, 1H), 3.50 – 3.34 (m, 5H), 3.16 (ddd, *J* = 29.6, 24.5, 15.1 Hz, 2H), 3.05 – 2.85 (m, 9H), 2.51 – 2.36 (m, 8H), 2.23 (d, *J* = 4.2 Hz, 2H), 1.64 – 1.54 (m, 6H), 1.53 – 1.46 (m, 3H), 1.43 (d, *J* = 7.1 Hz, 4H), 1.31 (d, *J* = 6.9 Hz, 2H). <sup>13</sup>C NMR (600 MHz, MeOD) δ = 174.15, 135.89, 130.46, 130.30, 129.03, 128.84, 57.72, 57.41, 49.67, 48.14, 44.70, 43.75, 43.37, 39.37, 37.65, 37.37, 34.93, 34.78, 33.61, 28.99, 25.67, 25.62, 24.87. LRMS (M + H)<sup>+</sup> : calcd for C<sub>17</sub>H<sub>26</sub>N<sub>2</sub>OS = 307.18, found 307.1

### Synthesis of MH6

0.126mmol of d-amphetamine sulfate was dissolved in 0.9mL of ethanol. 0.164mmol of 6-(tritylthio)hexyl methanesulfonate and 0.38mmol of potassium carbonate were added and the solution was heated to reflux overnight. After 14 hrs, ethanol was removed under vacuum and the residue dissolved in ethyl acetate. The organic layer was washed 2× with water, dried over sodium sulfate and rotovaped. The residue was then dissolved in 5mL of 10% TFA/DCM, and drops of TIS were added as a trityl scavenger. The solution was stirred for 1 hr and then rotovaped and purified by prep HPLC. Method = 0–5min 35%B, to 40%B over 2 min, to 44% B over 27min, to 95%B over 5 min, hold for 10min, requilibrate. Product retention time = 17min. Experimental Yield over 2 steps = 50%. <sup>1</sup>H NMR (600 MHz, MeOD) δ 7.31 (m, *J* = 7.5 Hz, 2H), 7.23 (m, 3H), 3.48 – 3.41 (m, 1H), 3.16 (dd, *J* = 13.2, 4.4 Hz, 1H), 3.07 – 2.97 (m, 2H), 2.66 (dd, *J* = 9.3, 3.9 Hz, 1H), 2.48 (t, *J* = 7.6 Hz, 1H), 1.73 – 1.55 (m, 4H), 1.47 – 1.35 (m, 4H), 1.17 (d, *J* = 6.6 Hz, 3H). <sup>13</sup>C NMR (600MHz, MeOD) δ = 137.32, 130.41, 130.03, 128.44, 56.95, 49.61, 46.31, 40.35, 39.22, 34.85, 29.88, 28.92, 28.82, 27.47, 27.26, 27.11, 24.79, 16.07. LRMS (M + H)<sup>+</sup> : calcd for C<sub>15</sub>H<sub>25</sub>NS = 252.17, found 252.2

### Synthesis of MH7 (4 steps)

**Synthesis of (S)-2,2,2-trifluoro-N-methyl-N-(1-(4-nitrophenyl)propan-2-yl)acetamide**—0.269mmol of d-methamphetamine hydrochloride were dissolved in 1.8mL DCM. 0.538mmol of triethyl amine were added and mixture was cooled to 0°C. 0.323mmol of trifluoroacetic anhydride were added dropwise and mixture was stirred at room temperature for 2.5 hrs. The solvent was removed under vacuum and residue dissolved in ethyl ether which incurred in the formation of a precipitate. The solution was passed through a short plug of silica topped with basic alumina. The filtrates were combined and rotovaped to yield a single spot by TLC which was carried forward without further purification. The residue was dissolved in 0.51mL DCM and added dropwise to a chilled solution consisting of 3.26mmol of potassium nitrate and 3.09mmol of concentrated sulfuric acid previously



dissolved in 1.63mL of DCM. The slurry was stirred overnight at room temperature. Aqueous solution of sodium sulfate was used to quench the reaction. The two layers were separated and the organic layer was washed twice more with aqueous sodium sulfate. Organics were combined, dried with anhydrous sodium sulfate and rotovaped. The product was purified using silica chromatography with 10% Ethyl acetate/hexane as the eluent. The major product of reaction was para- substituted as evidenced by NMR. Experimental Yield= 54% (para). TLC conditions 15% EtOAc/hex Rf = 0.16. Observe rotamers 1:0.5 by NMR, shifts and integration given for main rotamer. <sup>1</sup>H NMR (600 MHz, CDCl<sub>3</sub>) δ 8.17 (d, *J* = 8.7 Hz, 2H), 7.36 (d, *J* = 8.6 Hz, 2H), 4.87 (dq, *J* = 13.8, 6.9 Hz, 1H), 3.00 – 2.90 (m, 5H), 1.29 – 1.25 (m, 3H). <sup>13</sup>C NMR (600 MHz, CDCl<sub>3</sub>) δ = 176.84, 147.35, 147.20, 145.28, 144.79, 130.04, 129.90, 124.24, 124.05, 54.10, 52.40, 40.92, 39.50, 29.92, 29.37, 28.23, 18.49, 17.08. LRMS (M + H)<sup>+</sup> : calcd for C<sub>12</sub>H<sub>13</sub>F<sub>3</sub>N<sub>2</sub>O<sub>3</sub> = 291.09, found 291.4

#### **Synthesis of (S)-N-(1-(4-aminophenyl)propan-2-yl)-2,2,2-trifluoro-N-methylacetamide**

—0.174mmol of (S)-2,2,2-trifluoro-N-methyl-N-(1-(4-nitrophenyl)propan-2-yl)acetamide were dissolved in MeOH and 12mg of 10% activated palladium on carbon were added along with a hydrogen balloon. The reaction was stirred for 2 hrs before being filtered on a celite plug. The plug was washed with methanol, filtrates were combined and solvent was removed under vacuum. The residue was purified using silica chromatography using 20% Ethyl acetate/hexane as eluent. Experimental Yield= 97%. TLC conditions 30% EtOAc/hex Rf = 0.3. Observe rotamers by NMR 1: 0.7, shifts and integration given for main rotamer. <sup>1</sup>H NMR (500 MHz, CDCl<sub>3</sub>) δ 6.95 (d, *J* = 8.2 Hz, 2H), 6.66 – 6.59 (m, 2H), 4.82 – 4.70 (m, 1H), 3.60 (broad s, 2H), 2.92 (s, 3H), 2.83 – 2.62 (m, 2H), 1.29 – 1.17 (m, 3H). <sup>13</sup>C NMR (500 MHz, CDCl<sub>3</sub>) δ = 183.74, 145.33, 143.76, 130.13, 130.00, 127.62, 115.69, 115.63, 54.92, 53.03, 40.58, 38.97, 28.31, 18.17, 16.90. LRMS (M + H)<sup>+</sup> : calcd for C<sub>12</sub>H<sub>15</sub>F<sub>3</sub>N<sub>2</sub>O = 261.11, found 261.1

#### **Synthesis of (S)-N-(4-(2-(2,2,2-trifluoro-N-methylacetamido)propyl)phenyl)-6-(tritylthio)hexanamide**

—0.172mmol of (S)-N-(1-(4-aminophenyl)propan-2-yl)-2,2,2-trifluoro-N-methylacetamide were dissolved in 0.368mL DCM. 0.157 mmol of 6-(tritylthio)hexanoic acid, 0.204mmol of EDC, and 0.047mmol of DMAP were added and the mixture stirred. 0.314mmol of 4-methyl morpholine were added and reaction was stirred for 4hrs. 3mL of ethyl acetate were added and washed 2× with saturated sodium bicarbonate, 4× with 10% citric acid and 1× with water. The organic layer was dried over sodium sulfate and rotovaped to a yellow oil which corresponded to single spot on TLC. Experimental Yield= 93%. TLC conditions 20% EtOAc/hex Rf = 0.13. Observe amide rotamers at a ratio of 1: 0.63. <sup>1</sup>H NMR (600 MHz, CDCl<sub>3</sub>) δ 7.41 (dd, *J* = 12.7, 8.7 Hz, 13H), 7.27 (dd, *J* = 10.5, 4.3 Hz, 12H), 7.20 (t, *J* = 7.6 Hz, 4H), 7.16 – 7.04 (m, 5H), 4.85 – 4.73 (m, 1H), 2.91 (s, *J* = 25.0 Hz, 5H), 2.87 – 2.70 (m, 3H), 2.25 (dd, *J* = 12.1, 7.2 Hz, 3H), 2.16 (t, *J* = 6.9 Hz, 3H), 1.64 – 1.53 (m, 4H), 1.45 – 1.38 (m, 3H), 1.37 – 1.27 (m, 4H), 1.21 (t, *J* = 7.0 Hz, 7H). <sup>13</sup>C NMR (600 MHz, CDCl<sub>3</sub>) δ = 171.16, 145.14, 136.95, 136.73, 129.76, 129.67, 129.53, 128.02, 126.74, 120.19, 120.03, 66.65, 54.55, 52.67, 40.61, 39.01, 37.64, 31.92, 28.66, 28.63, 28.49, 28.18, 25.22, 18.08, 16.81. LRMS (M + Na)<sup>+</sup> : calcd for C<sub>37</sub>H<sub>39</sub>F<sub>3</sub>N<sub>2</sub>O<sub>2</sub>S = 655.25, found 655.3

#### **Synthesis of MH7**

0.145mmol of (S)-N-(4-(2-(2,2,2-trifluoro-N-methylacetamido)propyl)phenyl)-6-(tritylthio)hexanamide were dissolved in 1mL of methanol and drops of water. 0.436mmol of potassium carbonate were added and the mixture stirred at room temperature for 50hrs. The methanol was removed under vacuum and the residue was dropped in water. The aqueous layer was basified and extracted 3× with DCM. The organic layers were combined, dried over sodium sulfate and rotovaped. The residue was dissolved in 6mL of 10% TFA/

DCM and drops of TIS were added to scavenge the trityl groups. The solution was stirred for 1 hr and then rotovaped and purified by prep HPLC. Method = 0–5min 25%B, to 30%B over 2 min, to 40% B over 27min, to 95%B over 5 min, hold for 10min, requilibrate. Product retention time = 19min. Experimental Yield over 2 steps = 40%.  $^1\text{H}$  NMR (500 MHz, MeOD)  $\delta$  7.54 (dd,  $J$  = 8.6, 2.4 Hz, 2H), 7.21 (d,  $J$  = 8.5 Hz, 2H), 3.48 – 3.40 (m, 1H), 3.34 (s, 1H), 3.07 (dd,  $J$  = 13.7, 5.3 Hz, 1H), 2.71 (s, 3H), 2.51 (t,  $J$  = 7.6 Hz, 2H), 2.37 (t,  $J$  = 7.5 Hz, 2H), 1.74 – 1.61 (m, 4H), 1.52 – 1.45 (m, 2H), 1.23 (d,  $J$  = 6.6 Hz, 3H).  $^{13}\text{C}$  NMR (500 MHz, MeOD)  $\delta$  = 130.81, 121.84, 57.81, 39.71, 37.81, 34.88, 30.95, 28.95, 26.35, 24.83, 15.80. LRMS ( $M + H$ )<sup>+</sup> : calcd for  $\text{C}_{16}\text{H}_{26}\text{N}_2\text{OS}$  = 295.18, found 295.2

### Hapten-Protein Immunoconjugates

Immunoconjugates were prepared by reaction of the thiol presenting haptens with maleimide activated protein, either KLH or BSA. Briefly, protein activation was accomplished by reacting 1mg protein with 1mg of S-GMBS (*N*-[ $\gamma$ -maleimidobutyryloxy]sulfosuccinimide ester, Pierce) at a concentration of 5.4 mg protein/mL of EDC conjugation buffer. The solution was shaken at room temperature for 3 hrs and dialyzed thoroughly in order to remove unreacted material. The concentration of the activated solution was determined via the BCA assay. Pre-weighed haptens were then dissolved directly into the protein solution at a ratio of 0.5mg hapten: 1mg protein. The mixture is shook for 30min at room temperature followed by overnight shaking at 4°C. The solution is once again dialyzed and characterized. Coupling efficiencies were monitored using MALDI-TOF MS for all BSA conjugates. Due to the size of KLH, conjugates to this protein could not be directly analyzed. For BSA, all haptens showed similar coupling efficiencies of about 24–29 copies per BSA protein molecule.

### Vaccination Protocols for mice studies

Groups of  $n=4$  129G1<sup>x</sup> mice (6–8 weeks, 23–28g) were immunized i.p. on days 0, 14, and 35 with a suspension of each hapten-KLH conjugate (100  $\mu\text{g}$ ) in formulation with Sigma Adjuvant System (SAS, Sigma) according to the manufacturer's instructions. SAS is a stable oil-in-water emulsion that may be used as an alternative to the classical Freund's water-in-oil emulsions. This adjuvant is derived from bacterial and mycobacterial cell wall components such as detoxified Monophosphoryl Lipid A derived from *Salmonella minnesota* and synthetic Trehalose Dicorynomycolate that provide potent stimulus to the immune system. Following vaccine administration, serum (0.1 mL) was collected on days 21 and 42 via tail-bleed. All biological samples were stored at  $-80^\circ\text{C}$  until use to preserve integrity.

### Immunoassays: ELISA

Production of methamphetamine-specific IgG was initially monitored by ELISA using MH6- and MH7-BSA conjugates as the coating antigen. Titers were calculated from the plot of absorbance versus log dilution, and were defined as the dilution corresponding to an absorbance reading 50% of the maximal value. MH6-BSA, MH7-BSA and protein only controls were added individually to COSTAR 3690 microtiter plates and allowed to dry at 37°C overnight. Following methanol fixation, non-specific binding was blocked with a solution of 5% non-fat powdered milk in PBS for 0.5h at 37°C. Next, mouse sera was serially diluted in a 1% BSA solution across the plate and allowed to incubate for 1–2 hrs at 37°C in a moist chamber. Plates were then washed with DI H<sub>2</sub>O and treated with goat anti-mouse-HRP antibody for 0.5 hr at 37°C. Following another wash cycle, plates were developed with the TMB 2-step kit (Pierce; Rockford, IL).

## Equilibrium Dialysis

Refined values for antibody affinity, specificity and concentration were determined using a solution-based radioimmunoassay (RIA). A modified version of Muller's method<sup>29</sup> was followed as it allows for determination of both affinity constant and concentration of specific antibody in serum. The RIA was carried out in a 96-Well Equilibrium Dialyzer MWCO 5000 Da (Harvard Apparatus, Holliston, MA) to allow easy separation of bound and free (+)-[2',6'-<sup>3</sup>H(n)] methamphetamine tracer; specific activity = 39 Ci/mmol (obtained from the National Institute on Drug Abuse (Bethesda, MD) and synthesized at the Research Triangle Institute (Research Triangle Park, NC). Briefly, mouse sera for each bleed for each hapten was pooled together and diluted in RIA buffer (sterile filtered 2% BSA in 1× PBS pH=7.4) to a concentration that would bind 11–30% of ~24 000 decays/min of <sup>3</sup>H-methamphetamine tracer. A 100µL aliquot of sera was combined with 50µL of radiolabelled tracer (~24 000 decays/min) and 150µL of unlabeled competitor [(+)-methamphetamine or (+)-amphetamine] at varying concentrations in PBS pH=7.4 was added to the solvent chamber and the samples were allowed to reach equilibrium on a plate rotator (Harvard Apparatus, Holliston, MA) at room temperature for at least 22 hours. A 100µL aliquot from each sample/solvent chamber was slowly aspirated and suspended in 5mL scintillation fluid (Ecolite, ICN, Irvine, CA) and the radioactivity of each sample was determined by liquid scintillation spectrometry.

## Supplementary Material

Refer to Web version on PubMed Central for supplementary material.

## Acknowledgments

The authors thank the financial support provided by NIDA (DA024705) and The Skaggs Institute for Chemical Biology. (+)-[2',6'-<sup>3</sup>H(n)] methamphetamine for soluble radioimmunoassays was obtained from the National Institute on Drug Abuse (Bethesda, MD) and synthesized at the Research Triangle Institute (Research Triangle Park, NC).

## REFERENCES

1. Gonzales R, Mooney L, Rawson RA. The Methamphetamine Problem in the United States. *Annu. Rev. Public Health.* 2010; 31:385–98. [PubMed: 20070191]
2. Nicosia, N.; Pacula, RL.; Kilmer, B.; Lundberg, R.; Chiesa, J. The Economic Cost of Methamphetamine Use in the United States, 2005. RAND Corporation; Santa Monica, CA: 2009. <http://www.rand.org/pubs/monographs/MG829>
3. Treweek JB, Dickerson TJ, Janda KD. Drugs of Abuse That Mediate Advanced Glycation End Product Formation: A Chemical Link to Disease Pathology. *Accounts of Chemical Research.* 2009; 42(5):659–669. [PubMed: 19275211]
4. Meijler MM, Matsushita M, Wirsching P, Janda KD. Development of Immunopharmacotherapy Against Drugs of Abuse. *Curr. Drug Discovery Techn.* 2004; 1(1):77–89.
5. Karila L, Weinstein A, Aubin H-J, Benyamina A, Reynaud M, Batki SL. Pharmacological approaches to methamphetamine dependence: a focused review. *Br. J. Clin. Pharmacol.* 2010; 69(6):578–592. [PubMed: 20565449]
6. (a) Kantak KM. Vaccines against drugs of abuse: A viable treatment option? *Drugs.* 2003:341–352. [PubMed: 12558457] (b) Meijler M, Matsushita M, Wirsching P, Janda KD. Development of Immunopharmacotherapy Against Drugs of Abuse. *Curr. Drug. Discov. Technol.* 2004; 1:77–89. [PubMed: 16472221] (c) Kosten T, Owens SM. Immunotherapy for the treatment of drug abuse. *Pharmacol. Ther.* 2005; 108(1):76–85. [PubMed: 16023218]
7. (a) Cornuz J, Zwahlen S, Jungi WF, Osterwalder J, Klingler K, van Melle G, Bangala Y, Guessous I, Muller P, Willers J, Maurer P, Bachmann MF, Cerny T. A vaccine against Nicotine for Smoking Cessation: A Randomized Controlled Trial. *PLoS ONE.* 2008; 3(6):e2547. [PubMed: 18575629] (b)

- Hatsukami DK, Rennard S, Jorenby D, Fiore M, Koopmeiners J, de Vos A, Horwith G, Pentel PR. Safety and immunogenicity of a nicotine conjugate vaccine in current smokers. *Clin. Pharmacol. Ther.* 2005; 78(5):456–467. [PubMed: 16321612]
8. (a) Haney M, Gunderson EW, Jiang H, Collins ED, Foltin RW. Cocaine-specific antibodies blunt the subjective effects of smoke cocaine in humans. *Biol. Psychiatry.* 2010; 67(1):59–65. [PubMed: 19846066] (b) Martell BA, Orson FM, Poling J, Mitchell E, Rossen RD, Gardner T, Kosten TR. Cocaine vaccine for the treatment of cocaine dependence in methadone-maintained patients: a randomized, double-blind, placebo-controlled efficacy trial. *Arch. Gen. Psychiatry.* 2009; 66(10): 1116–1123. [PubMed: 19805702]
  9. Byrnes-Blake KA, Carroll FI, Abraham P, Owens SM. Generation of anti-(+)-methamphetamine antibodies is not impeded by (+) methamphetamine administration during active immunization of rats. *Int. Immunopharmacol.* 2001; 1:329–338. [PubMed: 11360933]
  10. Ino A, Dickerson TJ, Janda KD. Positional linker effects in haptens for cocaine immunopharmacotherapy. *Bioorg. Med. Chem. Lett.* 2007; 17(15):4115–4121.
  11. (a) Owens SM, Zorbas M, Lattin DL, Gunnell M, Polk M. Antibodies against arylcyclohexylamines and their similarities in binding specificity with the phencyclidine receptor. *J. Pharmacol. Exp. Ther.* 1988; 246(2):472–478. [PubMed: 2457075] (b) Matsushita M, Hoffman TZ, Ashley JA, Zhou B, Wirsching P, Janda KD. Cocaine catalytic antibodies: the primary importance of linker effects. *Bioorg. Med. Chem. Lett.* 2001; 11(2):87–90. [PubMed: 11206477]
  12. Peterson EC, Gunnell M, Che Y, Goforth RL, Carroll FI, Henry R, Liu H, Owens SM. Using Hapten Design to Discover Therapeutic Monoclonal Antibodies for Treating Methamphetamine Abuse. *J. Pharmacol. Exp. Ther.* 2007; 322:30–39. [PubMed: 17452421]
  13. Duryee MJ, Bevins RA, Reichel CM, Murray JE, Dong Y, Thiele GM, Sanderson SD. Immune response to methamphetamine by active immunization with peptide-based, molecular adjuvant-containing vaccines. *Vaccine.* 2009; 27:2981–2988. [PubMed: 19428909]
  14. Gentry WB, Ruedi-Bettschen D, Owens SM. Development of active and passive human vaccines to treat methamphetamine addiction. *Hum. Vaccin.* 2009; 5(4):206–213. [PubMed: 19276653]
  15. Kaminski GA, Friesner RA, Tirado-Rives J, Jorgensen WL. Evaluation and Reparametrization of the OPLS-AA Force Field for Proteins *via* Comparison with Accurate Quantum Chemical Calculations on Peptides. *J. Phys. Chem. B.* 2001; 105:6474–6487.
  16. Still WC, Tempczyk A, Hawley RC, Hendrickson TA. General Treatment of Solvation for Molecular Mechanics. *J. Am. Chem. Soc.* 1990; 112:6127–6129.
  17. Kolossváry I, Guida WC. Low-mode Conformational Search Elucidated. Application to C39H80 and Flexible Docking of 9-Deazaguanine Inhibitors to PNP. *J. Comput. Chem.* 1999; 20:1671.
  18. David, RL. *Handbook of Chemistry and Physics.* 90th ed.. CRC Press; New York, NY: 2009–2010. p. 2804
  19. Huizing G, Beckett A. Physico-chemical aspects of metabolically induced changes at the basic centre of two anti-emetics; relationship with *in vivo* membrane penetration. *Pharm. World Sci.* 1980; 2(1):253–261.
  20. Beaumont D, Waigh RD, Sunbhanich M, Nott MW. Synthesis of 1-(aminomethyl)-1,2,3,4-tetrahydroisoquinolines and their actions at adrenoceptors *in vivo* and *in vitro*. *J. Med. Chem.* 1983; 26(4):507–515. [PubMed: 6834382]
  21. Shelley J, Cholleti A, Frye L, Greenwood J, Timlin M, Uchimaya M. Epik: a software program for pK<sub>a</sub> prediction and protonation state generation for drug-like molecules. *Journal of Computer-Aided Molecular Design.* 2007; 21(12):681–691. [PubMed: 17899391]
  22. Meijler MM, Matsushita H, Atobell LJ, Wirsching P, Janda KD. A new strategy for improved nicotine vaccines using conformationally constrained haptens. *J. Am. Chem. Soc.* 2003; 125:7164–7165. [PubMed: 12797775]
  23. Dewey SL, Kroll C, Ferrieri R, Schiffer W, Alexoff D, Shea D, Youwen CX, Muench L, Volkow L, Fowler J. PET studies of methamphetamine enantiomers. *J. Nucl. Med. Meeting Abstracts.* 2006; 47:135P–b.
  24. (a) Mendelson J, Uemura N, Harris D, Nath R, Fernandez E, Jacob PI, Everhart ET, Jones RT. Human pharmacology of the methamphetamine stereoisomers. *Clin. Pharmacol. Ther.* 2006; 80(4):403–420. [PubMed: 17015058] (b) Wang Z, Woolverton WL. Estimating the relative

- reinforcing strength of ( $\pm$ )-3,4-methylenedioxymethamphetamine (MDMA) and its isomers in rhesus monkeys: comparison to (+)-methamphetamine. *Psychopharmacol.* 2007; 189(4):483–488.
25. Janda KD, Benkovic SJ, Lerner RA. Catalytic Antibodies with Lipase Activity and R and S Substrate Selectivity. *Science.* 1989; 244:437–440. [PubMed: 2717936]
26. Laurenzana EM, Hendrickson HP, Carpenter D, Peterson EC, Gentry WB, West M, Che Y, Carroll FI, Owens SM. Functional and biological determinants affecting the duration of action and efficacy of anti-(+)-methamphetamine monoclonal antibodies in rats. *Vaccine.* 2009; 27(50):7011–7020. [PubMed: 19800446]
27. Keyler DE, Roiko SA, Earley CA, Murtaugh MP, Pentel PR. Enhanced immunogenicity of a bivalent nicotine vaccine. *Int. Immunopharmacol.* 2008; 8:1589–1594. [PubMed: 18656557]
28. Carroll FI, Abraham P, Gong PK, Pidaparathi RR, Blough BE, Che Y, Hampton A, Gunnell M, Lay JO Jr, Peterson EC, Owens SM. The synthesis of haptens and their use for the development of monoclonal antibodies for treating methamphetamine abuse. *J. Med. Chem.* 2009; 52(22):7301–9. [PubMed: 19877685]
29. Muller R. Determination of affinity and specificity of anti-hapten antibodies by competitive radioimmunoassay. *Meth. Enzymol.* 1983; 92:589–601. [PubMed: 6190069]

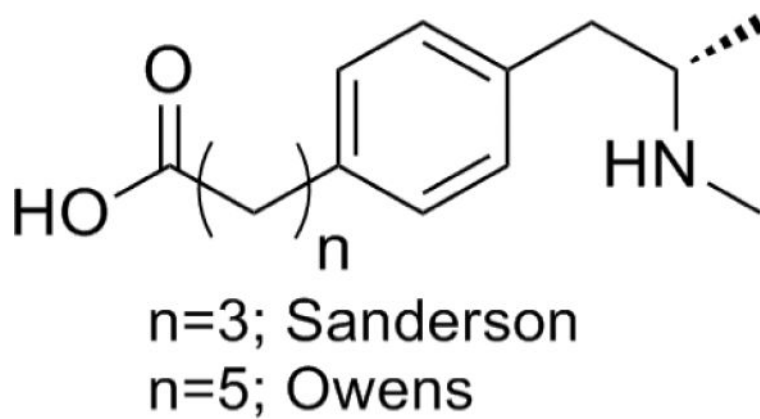


**Figure 1.**  
Previously reported haptens for active anti-METH vaccines.

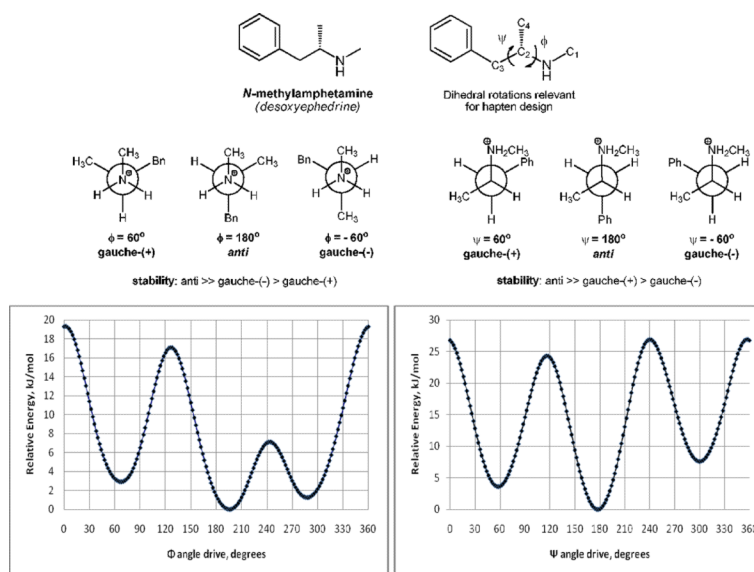


**Figure 2.** The conformational profile of *N*-methylamphetamine ( $\phi/\psi$ ), as determined by dihedral drive/OPLS\_2005-GB/SA simulations. Potential energy is expressed in relative terms to the following minima:  $-148.208$  kJ/mol ( $\Phi = 196^\circ$ ) and  $-148.197$  kJ/mol ( $\psi = 178^\circ$ ).

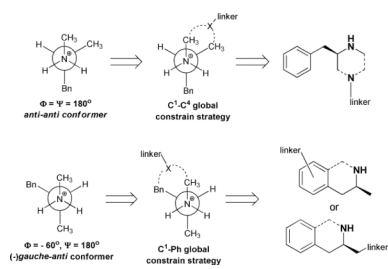


**Figure 3.**  
Two strategies toward conformationally constrained methamphetamine haptens.



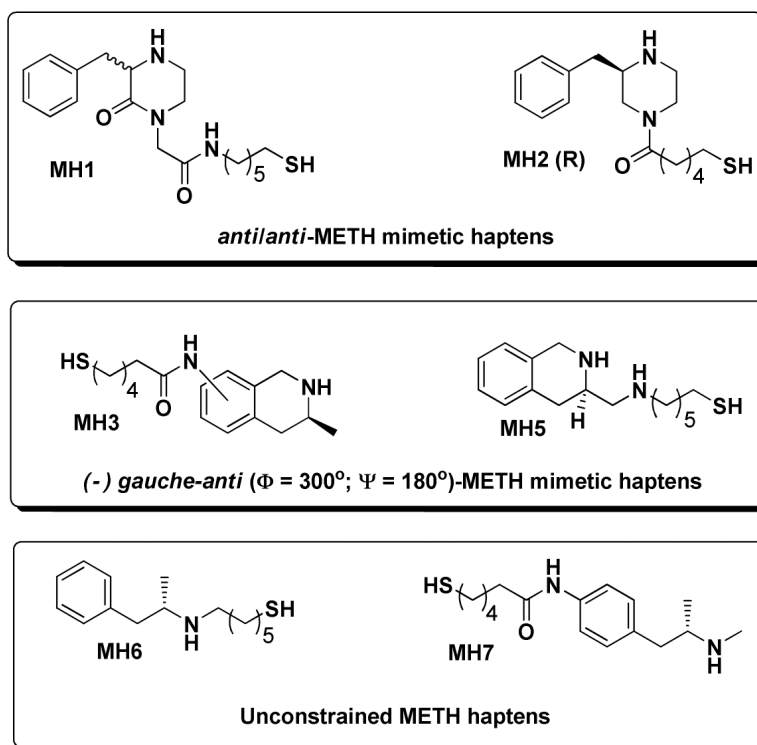


**Figure 4.**  
Designed hapten structures targeting (+)-methamphetamine.

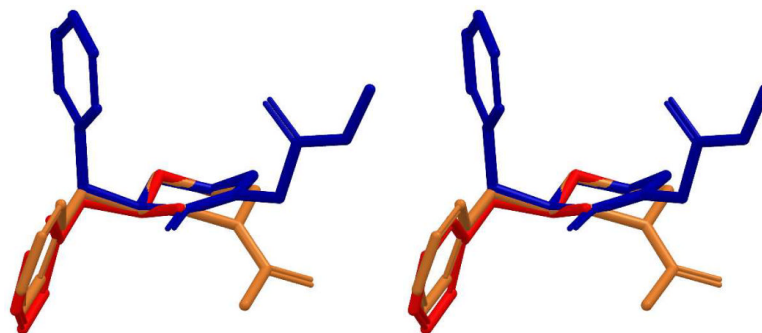


**Figure 5.** Stereoview of superposition of the global minima of (+)-methamphetamine (red), MH1 (blue) and MH2 (gold). RMSD (MH1-METH) = 0.15, RMSD (MH2-METH) = 0.11. Hydrogens are omitted for clarity.

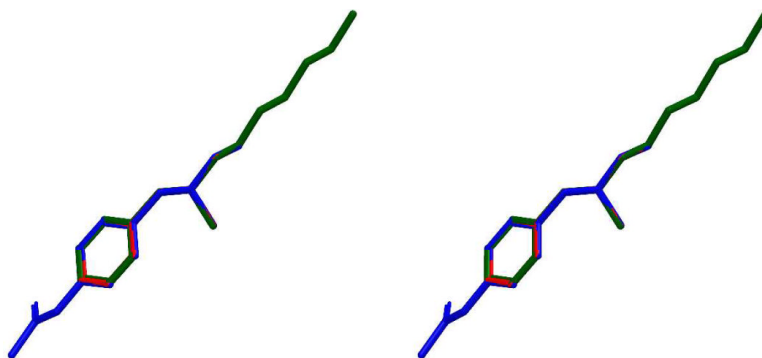


**Figure 6.** Stereoview of superposition of the global minima of (+)-methamphetamine (red), MH6 (green) and MH7 (blue). RMSD (MH6-METH) = 0.01, RMSD (MH7-METH) = 0.001. Hydrogens are omitted for clarity.

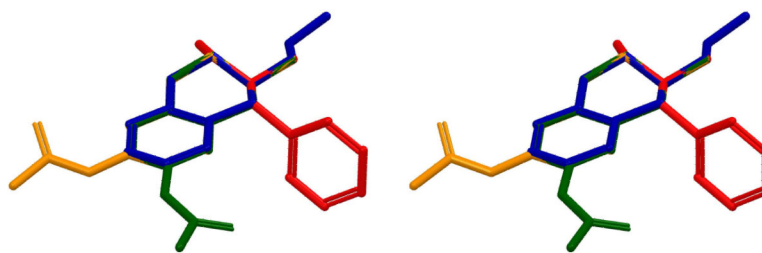


**Figure 7.** Stereoview of superposition of the (-)*gauche/anti* conformation of (+)-methamphetamine (red), and the global minima of two regio-isomers of MH3 (green and gold) and MH5 (blue). RMSD (MH3-METH) = 0.06, RMSD (MH5-METH) = 0.02. Hydrogens are omitted for clarity.

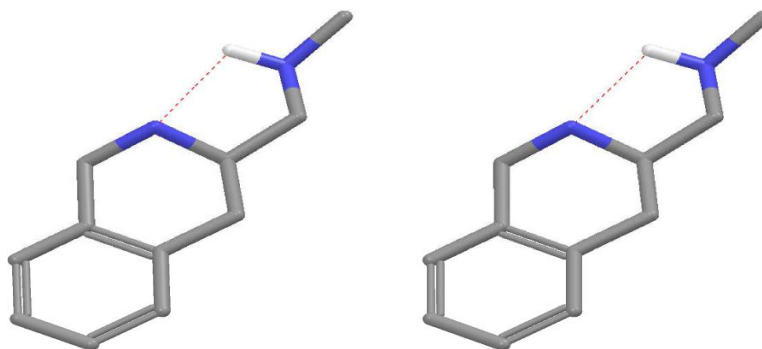
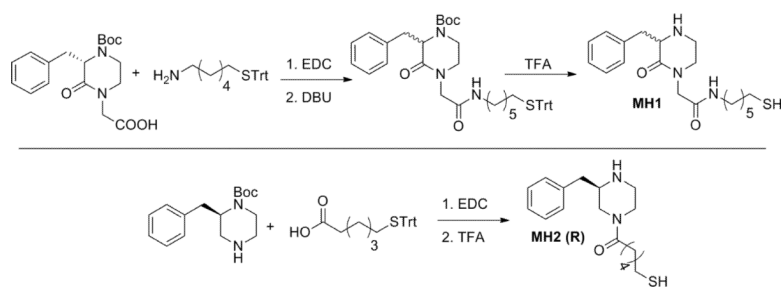
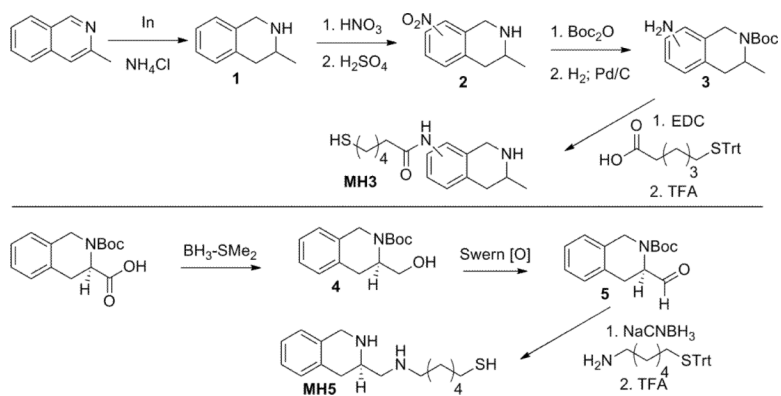


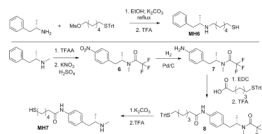
**Figure 8.** Stereoview of the global minimum of the protonated form of MH5, showing the putative intramolecular hydrogen bonding. Hydrogens are omitted for clarity.



**Scheme 1.**  
Synthesis of constrained *anti-anti* METH mimetic haptens, MH1/MH2.



**Scheme 2.**  
Synthetic routes towards (–) *gauche-anti* METH mimetic haptens, MH3/MH5.



**Scheme 3.**  
Synthetic routes towards unconstrained METH haptens, MH6/7.



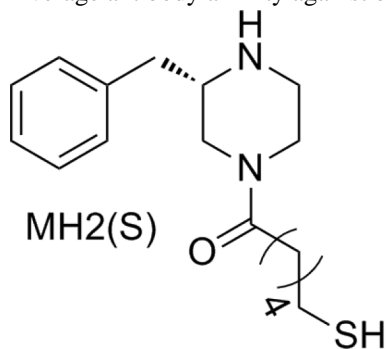
**Table 1**

Average relative affinities of antisera from immunized mice against amphetamine and methamphetamine as determined by equilibrium dialysis.

<b>Immunized Antigen</b>		<b>[Abs] <math>\pm</math> S.E. <math>\mu\text{g/mL}</math></b>	<b>(+)-METH <math>K_D(\mu\text{M})</math></b>	<b>(+)-amph <math>K_D(\mu\text{M})</math></b>
MH2 (R)	1rst bleed	70.83 $\pm$ 4.05	0.218 $\pm$ 0.055	1.267 $\pm$ 0.309
	2nd bleed	44.53 $\pm$ 2.54	0.082 $\pm$ 0.018	0.356 $\pm$ 0.093
MH6	1rst bleed	220.13 $\pm$ 19.69	0.266 $\pm$ 0.034	1.12 $\pm$ 0.171
	2nd bleed	107.83 $\pm$ 7.22	0.130 $\pm$ 0.019	0.724 $\pm$ 0.082
MH7	1rst bleed	152.53 $\pm$ 9.08	0.152 $\pm$ 0.011	23.73 $\pm$ 3.52
	2nd bleed	89.85 $\pm$ 11.89	0.169 $\pm$ 0.023	22.54 $\pm$ 4.70

**Table 2**

Average antibody affinity against both isomers of methamphetamine as determined by equilibrium dialysis.



Immunized Antigen		(+)-METH $K_D(\mu M)$	(-)-METH $K_D(\mu M)$
MH2 (S)	2nd bleed	1.720	0.276
MH6	1st bleed	0.266	3.050
	2nd bleed	0.130	2.010